



# Design of steel frames equipped with BRBs in the framework of Eurocode 8



M. Bosco<sup>a</sup>, E.M. Marino<sup>b,\*</sup>, P.P. Rossi<sup>b</sup>

<sup>a</sup> Department of Building, Civil and Environmental Engineering, Concordia University, 1455 de Maisonneuve Blvd. West, Montreal, Quebec, Canada

<sup>b</sup> Department of Civil Engineering and Architecture, University of Catania, v.le A. Doria 6, 95125 Catania, Italy

## ARTICLE INFO

### Article history:

Received 4 February 2015

Received in revised form 24 April 2015

Accepted 7 May 2015

Available online xxxx

### Keywords:

BRB

Steel structure

Behaviour factor

Seismic design

Eurocode 8

## ABSTRACT

Buckling restrained braces (BRBs) have been investigated extensively by means of experimental tests and their large ductility has been pointed out by many studies. Nevertheless, Eurocode 8 (EC8) does not provide any rules for design of steel frames with BRBs. For this reason, a design procedure for steel frames equipped with BRBs is proposed in this paper. The proposed design procedure is obtained by modifying the rules stipulated in EC8 for steel chevron braced frames. As a consequence, the obtained design procedure is consistent with the framework of EC8. BRBs are designed in terms of ductility and strength based on two parameters: the design storey drift  $\Delta u^d$ , i.e. the maximum accepted storey drift demand for earthquakes with a given probability of occurrence, and the behaviour factor  $q$ , which is a seismic force reduction factor correlated with the expected ductility of the structure. Beams and columns are designed according to capacity design principles derived from those given in EC8 with reference to steel chevron braced frames.

The design procedure is applied to a set of multi-storey frames with BRBs assuming different values of  $\Delta u^d$  and  $q$ . Their seismic response is evaluated by nonlinear dynamic analysis for two seismic excitation levels. The BRBs are modelled by a refined numerical model calibrated on the basis of a wide database of experimental data. For each value of  $\Delta u^d$ , the highest values of  $q$  leading to seismic response that does not exceed the Significant Damage and Near Collapse limit states are determined. Then, the suggested behaviour factor is given as a function of the design storey drift.

© 2015 Elsevier Ltd. All rights reserved.

## 1. Introduction

A buckling restrained brace (BRB) basically consists of a ductile steel core that is restrained from buckling and thus forced to yield both in tension and in compression [1,2]. Usually, the steel core is encased over its length in a steel tube filled with mortar (Fig. 1). A slip interface between the steel core and the surrounding mortar avoids the transfer of the axial force from the steel core to the casing and ensures that axial force is carried by the steel core only. On each ending part of the brace, the steel core is connected to the surrounding frame through two segments: the *connection segment*, which hosts the hole pattern, and the *transition segment*, which links up the steel core to the connection segment [2,3]. Both the transition segment and the connection segment behave elastically because their cross-sectional area is larger than that of the yielding core.

In the recent past, the cyclic behaviour of BRBs was investigated extensively by means of experimental tests [4–14]. These experiments showed stable hysteresis loops with nearly bilinear shapes, significant kinematic and isotropic hardening, similarly to other members that

dissipate energy by their hysteretic behaviour [15–17]. Because of strain hardening, the maximum tension force of BRBs is higher than the plastic resistance. In addition, the maximum force experienced in compression is slightly greater than that sustained in tension because of friction between the yielding core and the mortar jacket. The ductility capacity can be very high; in some experimental tests, BRBs subjected to cyclic loading sustained ductility demands close to 25 without failure [12].

Although the above mechanical properties have been confirmed by a number of research studies, the design of structures equipped with BRBs is ruled in American codes but not in some other codes, e.g. Eurocode 8 (EC8) [18]. For this structural type, the “NEHRP Recommended Provisions for Seismic Regulation for New Buildings and other Structures” (FEMA-450) [19] and the AISC 2005 “Seismic Provision for Structural Steel Buildings” [20] stipulate values of the *response modification coefficient*  $R$  equal to either 7 or 8 in the case of pinned or moment-resistant beam-to-column connections, respectively. Unfortunately, although the response modification factor is conceptually equivalent to the *behaviour factor*  $q$  in EC8, the design provisions given in the codes above cannot be directly transferred into the European code because the performance levels required by American and European codes are different.

Some research studies investigate the seismic response of steel frames with BRBs in order to suggest adequate values of the behaviour

\* Corresponding author. Tel.: +39 095 7382274.

E-mail address: emarino@dica.unict.it (E.M. Marino).

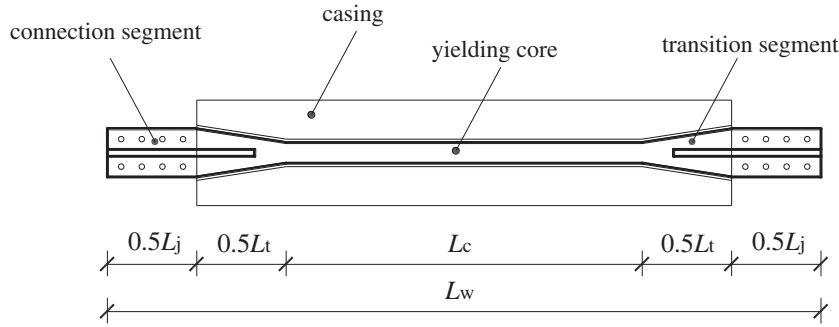


Fig. 1. Schematic representation of a BRB.

factor [21–25]. However, these studies refer to frames designed according to seismic codes different from EC8 (e.g. Iranian Earthquake Resistance Design Code or FEMA 302/303) and are sometimes carried out by means of pushover analysis [25], which is not always accurate in the prediction of the seismic response [26–28]. Moreover, the modelling adopted in these research studies for BRBs casts a shadow on the accuracy of the obtained results. In fact, BRBs are commonly modelled as elasto-plastic truss elements with kinematic hardening defined by means of a specified post-yield stiffness ratio. In some studies, the post-yield stiffness ratio is conservatively assumed equal to zero [21, 22, 29], while in others it is set equal to 1% or 2% [23, 25, 30, 31]. These latter values of the post-yield stiffness ratio are effective to avoid the numerical instability that may occur if a null value of the post-yield stiffness ratio is considered [32]. However, they still underestimate the effect of strain hardening in BRBs. Such a conservative choice of the value of the post-yield stiffness ratio leads to overestimate the displacement demand (maximum storey drift, residual drift and ductility demand of BRBs) but also to underestimate the axial force transmitted by BRBs to the frame. Therefore, it is not conservative for the verification of non-dissipative members. To mitigate this drawback, in some research studies the post-yield stiffness ratio is calibrated so that, for a reference ductility demand of the BRB, the ratio of the maximum tension force to the plastic resistance of the BRB is equal to that observed in experimental tests. This fictitious kinematic hardening also includes the effects of isotropic hardening. However, because of the saturation of the isotropic hardening of the BRBs at large deformations, it overestimates the BRB axial force for ductility demands larger than the reference value and underestimates residual drifts. The limitations of the elasto-plastic model with kinematic hardening can be overcome by more refined models of BRBs that consider explicitly the effect of isotropic hardening. One of these models has been proposed by Zona and Dall'Asta [33] and is now implemented in OpenSees [34]. The importance of modelling separately kinematic and isotropic hardening for a proper evaluation of seismic response of frames with BRBs was recently underlined in [32].

In this paper a design procedure for steel frames equipped with BRBs is proposed and a refined numerical modelling of BRBs is adopted to investigate its effectiveness. The proposed design procedure is obtained by modifying the rules stipulated in EC8 for steel chevron braced frames and thus is consistent with the framework of EC8. Two design parameters control the design procedure: the design storey drift  $\Delta u^d$ , which is related to the available ductility of the BRBs, and the behaviour factor  $q$ , which accounts for the trade-off between strength and ductility. A parametric analysis, based on multiple dynamic nonlinear analyses, is used to suggest a simple relation of proper values of the behaviour factor  $q$  as a function of the design storey drift  $\Delta u^d$ . The recommended values of  $q$  are determined from a performance-based design perspective. They ensure the Significant Damage and the Collapse Prevention performance levels defined in EC8 in occurrence of ground motions with probabilities of exceedance of 10% and 2% in 50 years, respectively. The model proposed by Zona and Dall'Asta [33] is used to simulate the

hysteretic cyclic response of BRBs. The parameters that control the model are determined based on the results of a set of experimental tests available in the literature [4, 10–12].

## 2. Proposed design procedure

As usual in practice, the modal response spectrum analysis is performed on a structural scheme in which all connections are pinned [35, 36]. The design spectrum is obtained reducing the elastic response spectrum by means of the behaviour factor  $q$ . The elastic response spectrum is that representative of ground motions with 10% probability of exceedance in 50 years [18] stipulated in EC8 for the Significant Damage verification [37]. The equations for the determination of the elastic and design spectra may be found in EC8 – Part 1 [18]. The BRBs are modelled as truss elements with equivalent cross-sectional area  $A_{eq}$

$$A_{eq} = \frac{A_c}{\frac{L_j}{L_w} \frac{A_c}{A_j} + \frac{L_t}{L_w} \frac{A_c}{A_t} + \frac{L_c}{L_w}} \quad (1)$$

where  $L_w$  is the work-point to work-point length,  $L_c$  and  $A_c$  are the length and cross-sectional area of the yielding core,  $L_j$  and  $A_j$  are the length and cross-sectional area of the two connection segments while  $L_t$  and  $A_t$  are the length and cross-sectional area of the two transition segments (Fig. 1). Note that generally the cross-section of each transition segment is not constant and an equivalent value of the area  $A_t$  representative of the whole segment has to be used. For instance, if the cross-sectional area of the transition segment varies linearly along its length,  $A_t$  is calculated as the average value of the cross-sectional areas of the two ends of the segment. The braces are designed on the basis of axial forces evaluated by modal response spectrum analysis. The design internal forces of beams and columns are evaluated in accordance with the capacity design principles by means of rules that are formally similar to those reported in EC8 for steel chevron braced frames.

### 2.1. Design of braces

The BRBs are designed for ductility and strength. The maximum ductility demand  $\mu_{max}$  that the BRBs can accommodate (ratio of the maximum elongation/shortening  $\delta_{max}$  to the yielding elongation  $\delta_y$ ) is a designer choice as long as it is compatible with BRB technology. In the proposed design procedure this choice is made once the design storey drift  $\Delta u^d$ , i.e. the maximum accepted storey drift demand for earthquakes with a given probability of occurrence, is assigned. According to the provisions of AISC 2005 on the qualifying cyclic tests of BRBs, the buckling–restraining system is required to sustain ductility demand corresponding to two times the design storey drift. The ductility demand of the BRB can also be calculated as the ratio of the contribution of the storey drift demand caused by the axial deformation of BRBs to the contribution corresponding to the BRB yielding. Based on this consideration and on the AISC requirement, the ductility capacity  $\mu_{max}$

can be determined at each storey as a function of the assigned  $\Delta u^d$ . The procedure described in reference [38] is used here for the calculation of  $\mu_{\max}$ . Preliminarily, the ductility demand of the BRBs of the  $i$ -th storey  $\mu_i$  corresponding to the design drift  $\Delta u^d$  is determined. To this end, the storey drift  $\Delta u_i$  produced by the design seismic forces is calculated. Since, in this study, the cross-sectional area assigned to BRBs is exactly equal to that required by the design seismic forces, the storey drift  $\Delta u_i$  is also equal to the yielding storey drifts  $\Delta u_i^y$ . Furthermore, the storey drift  $\Delta u_i$  can be evaluated as the sum of the contributions  $\Delta u_i^b$  and  $\Delta u_i^c$  due to the axial deformations of braces and columns, respectively. The two deformation contributions can be calculated as

$$\Delta u_i^b = \frac{A_{c,i} f_y L_w}{E A_{eq,i} \cos \alpha_b} \quad (2a)$$

$$\Delta u_i^c = \Delta u_i - \Delta u_i^b = \Delta u_i^y - \Delta u_i^b \quad (2b)$$

where  $\alpha_b$  is the angle of inclination of the brace with respect to the longitudinal axis of the beam. As the design storey drift  $\Delta u^d$  is larger than  $\Delta u_i$ , the BRBs undergo plastic deformations. When the yielding storey drift  $\Delta u_i^y$  is exceeded, the contribution provided by the axial deformations of the columns becomes negligible and the increase of the drift is

$$(\mu_i - 1) \cdot \Delta u_i^b = \Delta u^d - (\Delta u_i^b + \Delta u_i^c). \quad (3)$$

Finally, the ductility  $\mu_{\max,i}$  that the braces should possess is calculated so that the buckling-restraining system sustains deformations corresponding to two times those required by the design storey drift

$$\mu_{\max,i} = 2\mu_i = 2 \frac{\Delta u_i^d - \Delta u_i^c}{\Delta u_i^b}. \quad (4)$$

The minimum required cross-sectional area of the yielding core is obtained by equating the axial force  $N_{Ed}$  produced by the seismic design action to the axial resistance of the BRB, i.e.

$$A_{c,i} = \frac{N_{Ed,i}}{f_y \gamma_{M0}} \quad (5)$$

where  $f_y$  is the yield stress of the BRB core and  $\gamma_{M0}$  is the partial safety factor for resistance of cross-sections.

If necessary, the seismic internal forces obtained from the structural analysis are amplified to counteract  $P$ – $\Delta$  effects [39]. This amplification is stipulated on the basis of the value of the interstorey drift sensitivity coefficient  $\theta$  calculated by means of the relation

$$\theta_i = \frac{P_{\text{tot},i} \Delta u_i q}{V_i h} \quad (6)$$

where  $P_{\text{tot}}$  is the total gravity load at and above the  $i$ -th storey in the seismic design situation,  $V$  is the total seismic storey shear,  $h$  is the interstorey height and  $\Delta u$  is the storey drift provided by the design seismic forces at the storey under consideration. No amplification of the seismic action effects is required if  $\theta \leq 0.1$ ; instead, if  $0.1 < \theta \leq 0.2$ , the second order effects are taken into account by multiplying the seismic action effects by a factor equal to  $1 / (1 - \theta)$ . If  $\theta > 0.2$ , the simplified

approach is not applicable and a second order analysis has to be performed. In any case, the value of the parameter  $\theta$  cannot be greater than 0.3.

To promote a widespread yielding within the structure, the plastic resistance ( $N_{pl,Rd} = A_c f_y$ ) of the BRBs is such that, at each storey, the overstrength factor  $\Omega$  does not exceed the minimum value  $\Omega_{\min}$  by more than 25% of this minimum value. The overstrength factor  $\Omega$  is calculated at the storey under consideration as

$$\Omega_i = \frac{N_{pl,Rd,i}}{N_{Ed,i}}. \quad (7)$$

## 2.2. Design of non-dissipative members

The axial force on beams and columns is calculated as the sum of the axial force  $N_{Ed,G}$  due to the gravity load in the seismic design combination and the axial force produced by the seismic actions. This latter contribution is amplified with respect to the value  $N_{Ed,E}$  resulting from the structural analysis to account for strain hardening and overstrength of BRBs. In particular, it is calculated assuming that the buckling restrained braces with the minimum overstrength factor experience axial forces corresponding to the assumed maximum ductility demand of the braces. To evaluate the amplification above, the ratio of the maximum tension force to the plastic resistance is given by the tension strength adjustment factor  $\omega$  while the ratio of the maximum compression force to the plastic resistance is given by the product of the tension strength adjustment factor  $\omega$  and the compression strength adjustment factor  $\beta$ . In keeping with EC8, the internal axial force  $N_{Ed}$  of beams and columns is evaluated by means of the following relation

$$N_{Ed,i} = N_{Ed,G,i} + 1.1 \gamma_{ov} \frac{1 + \beta}{2} \omega^* \Omega_{\min} N_{Ed,E,i} \quad (8)$$

where  $\gamma_{ov}$  is the material overstrength factor and  $\omega^*$  is the tension strength adjustment factor at the storey where the overstrength factor  $\Omega$  is minimum.

Owing to the difference between the maximum forces in the braces in tension and in compression, an unbalanced vertical force  $P_{\text{unb}}$  develops during strong ground motions in the middle of the beam. This vertical force causes shear forces  $V_{Ed}^{(b)}$  and bending moments  $M_{Ed}^{(b)}$  on the beams. These internal forces cannot be directly evaluated by scaling the results of the design elastic analysis because the axial forces provided by this analysis are equal in the braces of a single storey. Owing to this, they are calculated in a manner similar to that proposed in EC8 for concentrically braced frames in the chevron configuration. In particular, the unbalanced vertical force  $P_{\text{unb}}$  is calculated at each storey by means of an equilibrium equation supposing that the axial force in the brace in tension is equal to  $1.1 \gamma_{ov} \omega_i N_{pl,Rd,i}$  and that of the brace in compression is  $1.1 \gamma_{ov} \beta \omega_i N_{pl,Rd,i}$

$$P_{\text{unb}} = 1.1 \gamma_{ov} (\beta - 1) \omega_i N_{pl,Rd,i} \sin \alpha_b. \quad (9)$$

**Table 1**

Properties of the BRBs tested by Black et al. (2002).

| Test  | $f_{ya}$<br>[MPa] | $A_c$<br>[mm <sup>2</sup> ] | $L_c$<br>[mm] | $L_w$ | $L_t$ | $L_j$ | $N^{(+)}$<br>[kN] | $N^{(-)}$ | $K_c$<br>[kN/mm] | $K_j$  | $K_w$ | $\delta^c$<br>[mm] |
|-------|-------------------|-----------------------------|---------------|-------|-------|-------|-------------------|-----------|------------------|--------|-------|--------------------|
| 99-1  | 418.50            | 2907                        | 3090          | 4500  | 550   | 860   | 1399              | –1518     | 197.5            | 3655.6 | 170.9 | 63.8               |
| 99-2  | 418.50            | 3876                        | 2990          | 4500  | 650   | 860   | 1853              | –1988     | 272.1            | 3655.6 | 221.5 | 62.0               |
| 99-3  | 418.50            | 5149                        | 3450          | 4500  | 0     | 1050  | 2550              | –2793     | 313.5            | 3655.6 | 267.6 | 71.4               |
| 00-11 | 285.40            | 7125                        | 3410          | 4500  | 0     | 1090  | 3005              | –3400     | 438.9            | 4326.9 | 364.8 | 70.1               |
| 00-12 | 285.40            | 7125                        | 3410          | 4500  | 0     | 1090  | 3084              | –3322     | 438.9            | 4326.9 | 364.8 | 70.1               |

**Table 2**

Results of the experimental tests by Merritt et al. (2003).

| Test |          |                    |            | 14th cycle of the standard loading protocol |           |          | Last cycle of the standard loading protocol |           |          |
|------|----------|--------------------|------------|---|-----------|----------|---|-----------|----------|
|      | $f_{ya}$ | $A_c$              | $\delta_y$ | $N^{(+)}$                                   | $N^{(-)}$ | $\delta$ | $N^{(+)}$                                   | $N^{(-)}$ | $\delta$ |
|      | [MPa]    | [mm <sup>2</sup> ] | [mm]       | [kN]  | [kN]      | [mm]     | [kN]  | [kN]      | [mm]     |
| 1D   | 267.52   | 6452               | 5.33       | 2344.2                                      | −2468.8   | 34.8     | 2757.9                                      | −3087.1   | 84.3     |
| 2D   | 267.52   | 6452               | 5.33       | 2362.0                                      | −2477.7   | 34.8     | 2762.3                                      | −3109.3   | 83.3     |
| 3D   | 306.82   | 10,323             | 6.71       | 3963.4                                      | −4114.6   | 32.3     | 4555.0                                      | −4973.1   | 88.9     |
| 4D   | 306.82   | 10,323             | 6.71       | 3994.5                                      | −4145.7   | 32.3     | 4586.1                                      | −5013.1   | 86.9     |
| 5D   | 267.52   | 14,920             | 5.97       | 5377.9                                      | −5622.6   | 30.0     | 6432.1                                      | −6970.4   | 79.2     |
| 6D   | 267.52   | 14,920             | 5.97       | 5355.7                                      | −5578.1   | 29.7     | 6427.7                                      | −6988.2   | 79.0     |
| 1    | 289.58   | 2449               | 6.99       | 894.1                                       | −969.7    | 42.93    | 1063.1                                      | −1521.3   | 109.22   |
| 2    | 289.58   | 3842               | 7.37       | 1352.3                                      | −1467.9   | 42.93    | 1663.6                                      | −2326.4   | 114.30   |
| 3    | 289.58   | 5381               | 7.72       | 1801.5                                      | −1970.6   | 43.69    | 2095.1                                      | −2602.2   | 87.12    |
| 4    | 272.34   | 8168               | 7.47       | 2829.1                                      | −3015.9   | 43.43    | 3442.9                                      | −4359.3   | 117.86   |
| 5    | 289.58   | 11,517             | 7.90       | 3883.3                                      | −4225.8   | 43.18    | 4888.6                                      | −6707.9   | 125.48   |
| 6    | 289.58   | 11,526             | 7.47       | 3918.9                                      | −4248.1   | 42.93    | 4813.0                                      | −6743.5   | 117.09   |
| 7    | 289.58   | 18,408             | 7.90       | 6080.7                                      | −6534.4   | 43.18    | 7099.4                                      | −8456.1   | 83.31    |
| 8    | 289.58   | 18,466             | 7.62       | 6174.1                                      | −6596.7   | 43.94    | 6979.3                                      | −8024.6   | 77.98    |

The shear force  $V_{Ed}^{(b)}$  and bending moment  $M_{Ed}^{(b)}$  produced by  $P_{unb}$  on the beam are equal to

$$V_{Ed,i}^{(b)} = \frac{1.1\gamma_{ov}(\beta-1)\omega_i N_{pl,Rd,i} \sin\alpha_b}{2} \quad (10)$$

$$M_{Ed,i}^{(b)} = \frac{1.1\gamma_{ov}(\beta-1)\omega_i N_{pl,Rd,i} \sin\alpha_b}{4} L \quad (11)$$

where  $L$  is the length of the braced span.

### 3. Tension and compression strength adjustment factors

To define the relation between the strength adjustment factors ( $\omega$  and  $\beta$ ) and the ductility demand, the results of a wide set of laboratory tests are analysed. Unfortunately, these results cannot be compared directly. In fact, the tension strength adjustment factor  $\omega$  is calculated in some studies with reference to the actual yield strength of the core and in some others with reference to the nominal brace yield stress. Further, the axial deformations of the BRBs are often measured with reference to different gauge lengths and may include or disregard the bracket deformation, the connection plate deformation and the bolt deformation including slippage. In addition, the BRBs are characterised by a different ratio of the yielding core length to the overall length and are subjected to different loading protocols.

For these reasons, simple rules are first defined to make the available data consistent. Specifically, the tension strength adjustment factor is calculated as the ratio of the tension force to the actual value of the axial yield force and is later referred to as  $\omega_a$ . The ductility demand is calculated with reference to the distance  $L_{Ref}$  between the centres of the hole patterns at each end of the specimen.

#### 3.1. Tests by Black et al. (2002)

In the study by Black et al. [4] five BRBs were tested under different loading protocols. The main data of the BRBs considered are listed in Table 1. In particular, the table reports the yield stress  $f_{ya}$  as obtained from coupon tests of the steel core material, the core cross-section area  $A_c$ , the lengths  $L_c$ ,  $L_w$ ,  $L_t$ , and  $L_j$ , the maximum tension force  $N^{(+)}$  and the maximum compression force  $N^{(-)}$  in the last loading cycle, the axial stiffness  $K_c$  of the core, the axial stiffness  $K_j$  of the connection segment, the axial stiffness  $K_w$  of the whole brace and the maximum axial elongation  $\delta^c$  of the core.

These values are used to evaluate some geometric and elastic characteristics that are not explicitly reported in the abovementioned study. Specifically, the axial stiffness  $K_t$  of the transition segment

and the areas  $A_t$  and  $A_j$  are determined by means of the following relations

$$K_t = \frac{2}{\frac{1}{K_w} - \frac{1}{K_c} - \frac{2}{K_j}} \quad (12)$$

$$A_t = \frac{K_t L_t}{E_s} \quad (13)$$

$$A_j = \frac{K_j L_j}{E_s} \quad (14)$$

where  $E_s$  is the modulus of elasticity of steel.

The yield elongation  $\delta_y$  and the elongation  $\delta$  are calculated with reference to the length  $L_{Ref}$  by means of the following relation

$$\delta_y = \frac{f_{ya}}{E_s} \left( L_c + \frac{A_c}{A_t} L_t + 0.5 \frac{A_c}{A_j} L_j \right) \quad (15)$$

$$\delta = \delta^c + \frac{N^{(+)}}{E_s} \left( \frac{L_t}{A_t} + 0.5 \frac{L_j}{A_j} \right). \quad (16)$$

Finally, the tension strength adjustment factor  $\omega_a$  and the compression strength adjustment factor  $\beta$  are calculated as

$$\omega_a = \frac{N^{(+)}}{A_c f_{ya}} \quad (17)$$

$$\beta = \frac{N^{(-)}}{N^{(+)}}. \quad (18)$$

#### 3.2. Tests by Merritt et al. (2003)

In the research studies by Merritt et al. [10,11], fourteen BRBs were tested. The data of six BRBs are reported in reference [10]: out

**Table 3**

Properties of the BRBs tested by Newell et al. (2006).

| Test   | $f_{ya}$ | $A_c$              | $A_t$  | $A_j$  | $L_c$ | $L_w$ | $L_t$ | $L_j$ | $\delta_y^1$ |
|--------|----------|--------------------|--------|--------|-------|-------|-------|-------|--------------|
|        | [MPa]    | [mm <sup>2</sup> ] |        |        | [mm]  |       |       |       | [mm]         |
| 1G, 2G | 258.55   | 7742               | 20,203 | 27,280 | 3366  | 6607  | 1927  | 1314  | 5.33         |
| 3G, 4G | 258.55   | 17,420             | 25,647 | 41,615 | 3369  | 6355  | 1372  | 1314  | 6.10         |

**Table 4**

Results of the experimental tests by Newell et al. (2006).

| Test | 14th cycle of the standard loading protocol |           |               | Last cycle of the standard loading protocol |           |               | Last cycle of the high-amplitude protocol |           |               |
|------|---|-----------|---------------|---|-----------|---------------|---|-----------|---------------|
|      | $N^{(+)}$                                   | $N^{(-)}$ | $\delta^{L1}$ | $N^{(-)}$                                   | $N^{(-)}$ | $\delta^{L1}$ | $N^{(+)}$                                 | $N^{(-)}$ | $\delta^{L1}$ |
|      | [kN]  | [kN]      | [mm]          | [kN]  | [kN]      | [mm]          | [kN]                                      | [kN]      | [mm]          |
| 1G   | 2873.6                                      | −2909.1   | 31.0          | 3260.5                                      | −3442.9   | 59.7          | 3656.4                                    | −4252.5   | 118.1         |
| 2G   | 2806.8                                      | −2855.8   | 30.7          | 3193.8                                      | −3420.7   | 59.2          | 3580.8                                    | −4568.3   | 113.5         |
| 3G   | 6236.4                                      | −6289.8   | 34.3          | 6948.1                                      | −7206.1   | 63.5          | 7757.7                                    | −8407.1   | 116.8         |
| 4G   | 6303.1                                      | −6205.3   | 32.8          | 7046.0                                      | −7166.1   | 63.0          | 8091.3                                    | −9043.2   | 135.1         |

of these six braces, two (labelled 1D and 2D) have a flat core plate while the others (3D to 6D) have a cruciform core plate. The eight BRBs considered in [11] have a yielding segment consisting of flat core plates. In all the cases, the axial deformations are measured with a gauge length equal to  $L_{Ref}$ . Therefore, no manipulation of the data is necessary.

Table 2 shows the data that are useful to calculate the tension strength adjustment factor  $\omega_a$  and the ductility demand. To show data corresponding to different levels of the ductility demand, the results at the 14th cycle and at the last cycle of the standard loading protocol are reported.

### 3.3. Tests by Newell et al. (2006)

Four BRBs were tested in the research study by Newell et al. [12]. Two BRBs have a flat core plate (specimens 1G and 2G) while two BRBs have a cruciform core plate. The axial deformation was measured on a length  $L_1$  that includes the length of the yielding core and that of the transition segment. The geometric properties of these BRBs, the actual yield strength of the adopted steel and the axial deformation at yield  $\delta_y^{L1}$  are reported in Table 3. The values of the axial deformation  $\delta^{L1}$  achieved at three different cycles are reported in Table 4. Specifically, the results refer to the 14th cycle, to the last cycle of the standard loading protocol and to the last cycle of the high-amplitude protocol. The values of the maximum tension and compression forces achieved at these cycles are also reported.

On the basis of these data, the yield elongation  $\delta_y$  of a length  $L_{Ref}$  is calculated as the sum of  $\delta_y^{L1}$  and the elastic deformation caused by the axial yield force on half the connection segment. The following relation is obtained

$$\delta_y = \delta_y^{L1} + \frac{f_{ya} A_c L_j}{E_s A_j 2}. \quad (19)$$

Similarly, the elongation  $\delta$  is calculated as

$$\delta = \delta^{L1} + \frac{N^{(+)} L_j}{E_s A_j 2}. \quad (20)$$

Once again, the tension strength adjustment factor  $\omega_a$  and the compression strength adjustment factor  $\beta$  are calculated by Eqs. (17) and (18).

### 3.4. Analysis of the results

The obtained values of  $\omega_a$  are represented in Fig. 2a as a function of the corresponding values of the ductility demand  $\mu (= \delta/\delta_y)$ . Circles of different colours are adopted to represent results obtained in different studies while square symbols are used to highlight the experiments in which a high amplitude loading protocol has been considered. In the same figure, a straight line is also plotted which represents the equation proposed by the writers to correlate the tension strength adjustment factor  $\omega_a$  and the ductility demand  $\mu$

$$\omega_a = 1.15 + k_h(\mu - 1) \quad (21)$$

where  $k_h$  is the post-yield stiffness ratio which accounts for the kinematic hardening and is set equal to 3.16%. According to this equation, because of the isotropic hardening, the tension strength adjustment factor corresponding to  $\mu = 1$  is equal to 1.15.

Fig. 2b shows the values of the compression strength adjustment factor  $\beta$  as a function of the ductility demand  $\mu$ . With the exception of the specimens tested in [11],  $\beta$  moderately increases with  $\mu$  and ranges from 1.0 to 1.2. As a simplification, a  $\beta$  value equal to 1.1 appears to be proper to simulate the behaviour of BRBs and is accepted here as representative of the response of the BRBs adopted for design.

## 4. Analysed buildings

The proposed design procedure is applied to a simple building that is supposed to be used for apartments and is characterised by both geometric and mass properties equal at all storeys. To test the design procedure also with reference to systems in which higher modes of vibration may affect the structural behaviour significantly, the buildings are assumed to have four, eight or twelve storeys. The structural scheme is defined by the intersection of two sets of four plane frames disposed along two orthogonal directions with three spans each (Fig. 3). The frames located along the perimeter are

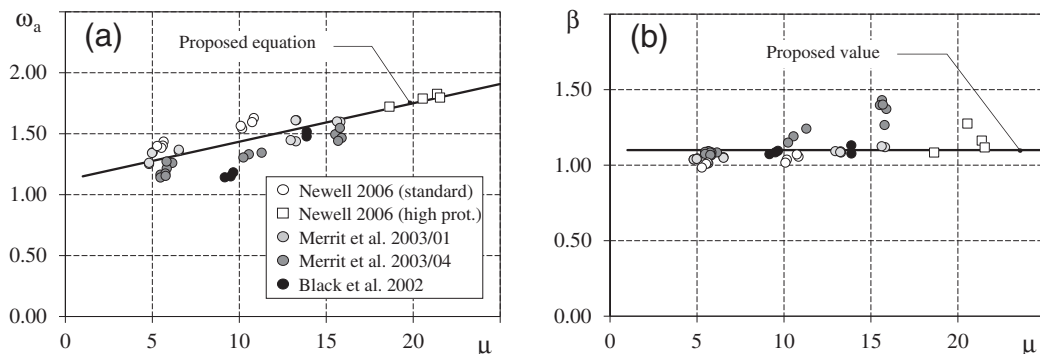


Fig. 2. (a) Tension and (b) compression strength adjustment factors as a function of ductility.

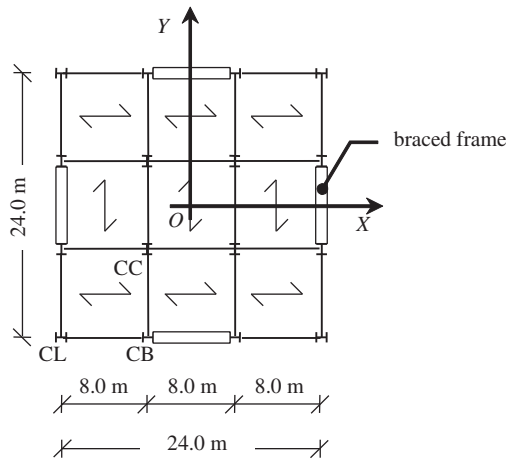


Fig. 3. Layout of the analysed buildings.

endowed with BRBs. These braces are arranged in the chevron configuration in the central span of the frame and are designed to sustain the entire seismic force of the building. The columns belonging to the braced frames, named CB type columns, are oriented with their strong axis orthogonal to the plane of the braced frame. The gravity columns are indicated by symbols CL and CC and are oriented with their strong axis orthogonal to the X-direction and Y-direction, respectively (Fig. 3). All the beam-to-column connections and column-to-base connections are assumed to be pinned.

The earthquake motion at the site under examination is represented by the elastic response spectrum proposed in EC8 for soft soil (type C) and is characterised by a design peak ground acceleration  $a_g$  equal to 0.35 g. The design spectrum is derived according to EC8 by means of the behaviour factor  $q$ . Masses are calculated on the basis of a mean value of the gravity loads equal to 5.0 kN/m<sup>2</sup>. The gravity load present on the floors in the non-seismic design situation is assumed equal to 9.16 kN/m<sup>2</sup>.

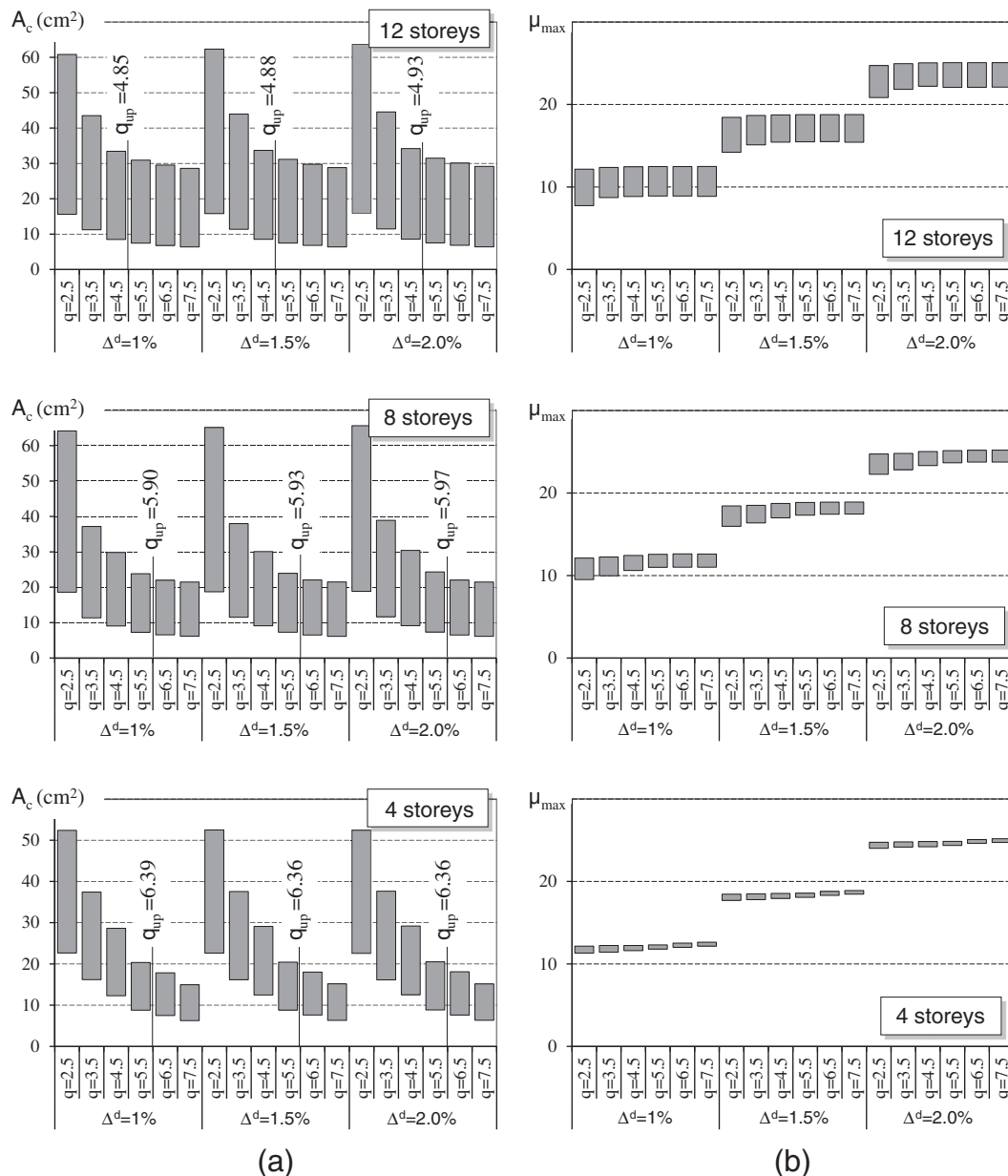


Fig. 4. (a) Cross-section area of the core of the braces; (b) ductility of the braces.

## 5. Design of the buildings

The buildings are designed by means of values of  $q$  ranging from 2.5 (suggested in EC8 for conventional chevron braced frames) to 7.5 in steps of 1.0. In addition, three values of the design storey drift  $\Delta u^d$  are considered to investigate different levels of the ductility capacity of the BRBs. Specifically, the ratio  $\Delta^d$  of the design storey drift to the interstorey height (later named *design storey drift angle*) is fixed equal to either 1.0%, 1.5% or 2.0%.

The length of the yielding core of the BRBs is assumed equal to  $0.5 L_w$ . As considered in Tremblay et al. [40], the length of each connection segment ( $L_j/2$ ) is equal to 650 mm. The length of the transition segment ( $L_t/2$ ) is equal to the difference between the work-point to work-point length of the brace and the sum of the lengths of the yielding core and connection segment, i.e.  $L_t/2 = 0.5 (L_w - L_c - L_j)$ . The cross-sectional areas of the connection and transition segments are assigned as a function of the cross-sectional area of the core by means of the ratios  $A_c/A_t = 0.5$  and  $A_c/A_j = 0.3$ .

The area of the yielding core of the braces is calculated by Eq. (5) assuming that the yield stress  $f_y$  is equal to 235 MPa (steel grade S235) and  $\gamma_{M0}$  is equal to 1. For each designed frame, Fig. 4a and b shows the minimum and the maximum required values of the cross-sectional area of the core  $A_c$  and the ductility capacity  $\mu_{max}$ . The minimum values of  $A_c$  and  $\mu_{max}$  are required at the top storey while the maximum values are required at the first storey. The average value of the cross-section areas of the yielding core along the height of the building ( $\bar{A}_c$ ) is virtually independent of the design storey drift angle but decreases with the increase in the behaviour factor. The reduction of  $\bar{A}_c$  per unit increase in the behaviour factor can be estimated as

$$\Delta \bar{A}_c = \frac{\bar{A}_{c,q} - \bar{A}_{c,q-1}}{\bar{A}_{c,q-1}} \quad (22)$$

where  $\bar{A}_{c,q}$  and  $\bar{A}_{c,q-1}$  are the average values of the cross-section areas corresponding to behaviour factors equal to  $q$  and  $(q - 1)$ , respectively. The variation of  $\Delta \bar{A}_c$  decreases with the increase in the behaviour factor and is very low for high values of the behaviour factor because in the design spectrum of EC8 the pseudo-acceleration cannot be lower than  $0.2a_g$ . A vertical line is plotted in Fig. 4a to identify the value of the behaviour factor  $q^{up}$  that corresponds to a reduction  $\Delta \bar{A}_c$  equal to 15%. This value of the behaviour factor is considered in the following proposal of the behaviour factor as an upper bound because the adoption of higher behaviour factors does not help to decrease the size of the structural members significantly.

The required ductility capacity is mainly related to the storey drift angle (Fig. 4b). The values of the ductility capacity obtained from the assigned storey drift angle are not uniform in elevation because the storey drift is due not only to the axial deformation of the braces but also to the axial deformation of the columns. In particular, this latter contribution increases with the height of the frame [38].

The cross-section area of the core and the ductility capacity assumed in this paper for braces are those that are strictly required in design. Owing to this, the brace overstrength factor  $\Omega$  is equal to 1 at each storey of the building. The tension adjustment factor is not constant in elevation because the ductility capacities resulting from design are not equal along the height of the building. The differences are, however, negligible and the average value of the tension strength adjustment factors is adopted here for design of columns of the braced frames.

The cross-section of these beams and columns is generally selected among the European wide flange sections (HEA for the beams, HEB or HEM for the columns) in such a way that the stability verification specified in Eurocode 3 (EC3) [41] is fulfilled. Compound sections, obtained from two IPE sections welded to the web of a HEB or HEM section, are used only sometimes in the lower storeys of the braced frames designed with low values of the behaviour factor. The partial safety coefficient for resistance of members to instability

**Table 5**

Member sizes of the 8-storey frames designed by  $\Delta^d = 1.5\%$  and different values of  $q$ .

|                                 | Storey | $q = 2.5$        | $q = 3.5$        | $q = 4.5$        | $q = 5.5$        | $q = 6.5$        | $q = 7.5$        |
|---------------------------------|--------|------------------|------------------|------------------|------------------|------------------|------------------|
| BRB $A_c$<br>(cm <sup>2</sup> ) | 8      | 18.72            | 11.51            | 9.09             | 7.29             | 6.51             | 6.13             |
|                                 | 7      | 30.74            | 18.20            | 14.44            | 11.52            | 10.46            | 10.07            |
|                                 | 6      | 39.66            | 22.74            | 18.10            | 14.35            | 13.26            | 13.03            |
|                                 | 5      | 46.85            | 26.39            | 21.02            | 16.58            | 15.52            | 15.41            |
|                                 | 4      | 53.08            | 29.85            | 23.80            | 18.77            | 17.59            | 17.51            |
|                                 | 3      | 58.43            | 33.21            | 26.47            | 20.88            | 19.47            | 19.33            |
|                                 | 2      | 62.64            | 36.11            | 28.76            | 22.83            | 21.13            | 20.74            |
|                                 | 1      | 65.13            | 37.99            | 30.09            | 23.94            | 22.05            | 21.49            |
| Beams                           | 8      | HEA 300          | HEA 240          | HEA 220          | HEA 220          | HEA 200          | HEA 200          |
|                                 | 7      | HEA 360          | HEA 280          | HEA 260          | HEA 240          | HEA 240          | HEA 240          |
|                                 | 6      | HEA 400          | HEA 320          | HEA 280          | HEA 260          | HEA 260          | HEA 240          |
|                                 | 5      | HEA 450          | HEA 340          | HEA 300          | HEA 280          | HEA 260          | HEA 260          |
|                                 | 4      | HEA 500          | HEA 360          | HEA 320          | HEA 280          | HEA 280          | HEA 280          |
|                                 | 3      | HEA 550          | HEA 400          | HEA 320          | HEA 300          | HEA 300          | HEA 280          |
|                                 | 2      | HEA 550          | HEA 400          | HEA 340          | HEA 300          | HEA 300          | HEA 300          |
|                                 | 1      | HEA 600          | HEA 400          | HEA 360          | HEA 320          | HEA 300          | HEA 300          |
| Columns                         | 8      | HEB 180          | HEB 160          | HEB 160          | HEB 160          | HEB 160          | HEB 160          |
|                                 | 7      | HEB 180          | HEB 160          | HEB 160          | HEB 160          | HEB 160          | HEB 160          |
|                                 | 6      | HEB 320          | HEB 260          | HEB 240          | HEB 220          | HEB 220          | HEB 220          |
|                                 | 5      | HEB 320          | HEB 260          | HEB 240          | HEB 220          | HEB 220          | HEB 220          |
|                                 | 4      | HEM              | HEB              | HEB              | HEB              | HEB              | HEB              |
|                                 |        | 320 <sup>a</sup> | 340 <sup>a</sup> | 300 <sup>a</sup> | 260 <sup>a</sup> | 260 <sup>a</sup> | 260 <sup>a</sup> |
|                                 | 3      | HEM              | HEB              | HEB              | HEB              | HEB              | HEB              |
|                                 |        | 320 <sup>a</sup> | 340 <sup>a</sup> | 300 <sup>a</sup> | 260 <sup>a</sup> | 260 <sup>a</sup> | 260 <sup>a</sup> |
|                                 | 2      | HEM              | HEB              | HEB              | HEB              | HEB              | HEB              |
|                                 |        | 400 <sup>b</sup> | 450 <sup>b</sup> | 400 <sup>a</sup> | 340 <sup>a</sup> | 320 <sup>a</sup> | 320 <sup>a</sup> |
|                                 | 1      | HEM              | HEB              | HEB              | HEB              | HEB              | HEB              |
|                                 |        | 400 <sup>b</sup> | 450 <sup>b</sup> | 400 <sup>a</sup> | 340 <sup>a</sup> | 320 <sup>a</sup> | 320 <sup>a</sup> |

Steel grade S235.

<sup>a</sup> Steel grade S275.

<sup>b</sup> Steel grade S355.

$\gamma_{M1}$  is assumed equal to 1. Steel grade S235 is used for all the beams while steel grade S235, S275 ( $f_y = 275$  MPa) or S355 ( $f_y = 355$  MPa) is used for the columns. According to common design practice, the same column cross-section is adopted for two consecutive storeys. Table 5 reports the sizes adopted for the BRBs (cross-sectional area of the core), the beams and the columns of the 8-storey frames designed by  $\Delta^d = 1.5\%$  and different values of  $q$ .

The gravity columns are designed to sustain gravity loads only. The axial force on the column is evaluated according to the tributary area concept. No bending moment is considered because all beam-to-column connections are pinned. The column cross-section is selected so that the buckling axial strength in the weak axis plane is not lower than the design axial force. Table 6 reports the cross-section adopted for the gravity columns of the 8-storey buildings.

## 6. Modelling

The numerical analyses are carried out by a two-dimensional model that represents half of the building. This simplification is possible because of the symmetry of the structure and because no eccentricity of the centre of mass is considered. The model includes the frame with

**Table 6**

Size of the gravity columns of the 8-storey buildings.

| Storey | CC column            | CL column            |
|--------|----------------------|----------------------|
| 8      | HEB 200              | HEB 160              |
| 7      | HEB 200              | HEB 160              |
| 6      | HEB 280              | HEB 160              |
| 5      | HEB 280              | HEB 160              |
| 4      | HEB 360 <sup>a</sup> | HEB 180 <sup>a</sup> |
| 3      | HEB 360 <sup>a</sup> | HEB 180 <sup>a</sup> |
| 2      | HEB 400 <sup>a</sup> | HEB 200 <sup>a</sup> |
| 1      | HEB 400 <sup>a</sup> | HEB 200 <sup>a</sup> |

Steel grade S235.

<sup>a</sup> Steel grade S275.

BRBs and six columns that are pinned at the base. The same steel profile is used to make the column for two consecutive storeys and it is joined to the subsequent one by rigid and full-strength or nominally pinned column-to-column connections. These two hypotheses on columns represent the two bounds of the column with actual semi-rigid connections with rotational stiffness that depends on the detailing. They are herein-after referred as *continuous column*, in the case of rigid and full-strength connections that make the column continuous for the whole height of the building, and *non-continuous column* in the case of nominally pinned column connections. The two types of columns are considered to evaluate the effect of the continuity of columns, especially with regard to residual drifts. In fact, previous studies have proved that the presence of continuous columns can reduce maximum and residual drift demands [42,43] and promote a more uniform distribution of drift demands along the height of the building [44,45] although this beneficial impact is counterbalanced by an increase in the bending moments of the columns [45].

Beams and columns of the braced frames and gravity columns are modelled as elastic beam-column elements, while BRBs are modelled as inelastic truss members. These latter members are characterised by the equivalent cross-section area  $A_{eq}$  and by the uniaxial material model proposed by Zona and Dall'Asta [33]. This model allows a gradual variation of the axial stiffness of the brace and considers both kinematic and isotropic hardening. It has been preferred to simpler bilinear models because, as proved in a recent paper [32], the structural response predicted by means of smoothed models incorporating isotropic and kinematic hardening may be sometimes quite different from that resulting from bilinear models. The full description of the uniaxial material proposed in [33] requires that values be assigned to the following parameters: the initial elastic stiffness ( $k_0$ ), the post-yield stiffness ( $k_1$ ), the yield stress ( $F_y$ ), the maximum yield stress in tension for the fully saturated isotropic hardening condition ( $F_{y,max}$ ) and the maximum yield stress in compression for the fully saturated isotropic hardening condition ( $F_{y,min}$ ), the coefficient  $\delta$  which rules the rate of the isotropic hardening and the coefficient  $\alpha$  which controls the trend of the transition from the elastic to the plastic response. In keeping with the results of Section 3 [Eq. (21)] and suggestions by Zona and Dall'Asta, the parameters above are fixed as follows

$$k_0 = E, k_1 = k_h k_0 \quad (23)$$

$$F_y = f_y \frac{A_c}{A_{eq}}, F_{y,max} = 1.15 F_y, F_{y,min} = 1.15 \beta F_y \quad (24)$$

$$\delta = 0.20, \alpha = 0.6. \quad (25)$$

## 7. Nonlinear dynamic analyses

Nonlinear dynamic analyses are carried out to investigate the fulfilment of the two target performance levels considered in EC8: the Significant Damage and the Near Collapse limit states. According to EC8, these two performance levels should not be exceeded during ground motions with probabilities of exceedance of 10% and 2% in 50 years. In this paper, the design parameters  $q$  and  $\Delta^d$  are calibrated in accordance with performance-based design principles. In particular, for each considered value of  $\Delta^d$ , the highest values of  $q$  corresponding to the achievement of the abovementioned performance objectives are determined. Then, the lowest value of these behaviour factors is proposed for design.

The seismic performance of the frames is investigated supposing that the ground motion input acts along the Y-axis (see Fig. 3). The seismic response of all the designed structures is evaluated by means of the OpenSees computer program [34] and taking into account  $P-\Delta$  effects. The Rayleigh formulation is used to introduce damping. Mass and stiffness coefficients are defined so that the first and second modes of vibration are characterised by an equivalent viscous damping ratio equal to 0.03. No stiffness proportional damping is considered for the braces, as assumed by other researchers for yielding elements [46].

### 7.1. Seismic input

The seismic input consists of two sets of accelerograms corresponding to probabilities of exceedance of 10% and 2% in 50 years. Specifically, the seismic events with 10% probability of exceedance are simulated by means of the twenty ground motions [47] adopted in the FEMA/SAC project. The response spectra of the SAC ground motions and their average spectrum are shown in Fig. 5a. In keeping with the spectrum-compatibility conditions of EC8, all these accelerograms are scaled here by a factor equal to 0.88 so as to match the 5% damped elastic response spectrum of EC8 for the soil type C and peak ground acceleration ( $a_g = 0.35$  g) assumed in design. Fig. 5b shows that the average spectrum of the scaled SAC ground motions is always very close to the elastic spectrum of EC8 for the whole range of fundamental periods covered by the analysed structures.

The other set of accelerograms, representative of seismic events with 2% probability of exceedance in 50 years, is obtained by scaling the accelerograms with 10% probability of exceedance. The scale factor ( $SF$ ) used here is equal 1.71 and is calculated by means of the following relation derived from the EC8 provisions [37]

$$SF = \left( \frac{P_{LR}}{P_L} \right)^{\frac{1}{2}} \quad (26)$$

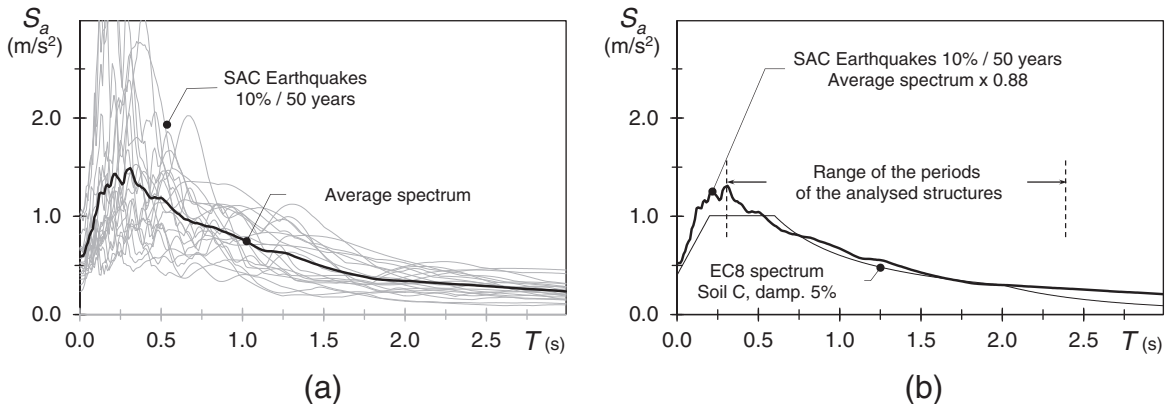


Fig. 5. (a) Response spectra of SAC accelerograms; (b) comparison of the average spectrum of scaled SAC accelerograms and EC8 spectrum.

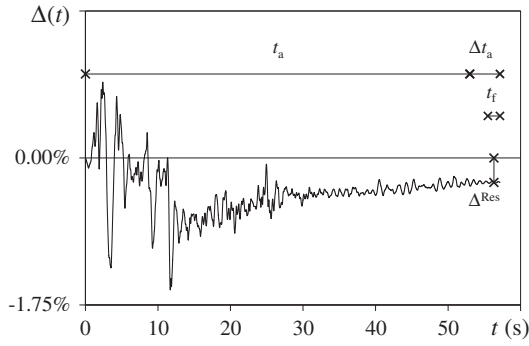


Fig. 6. Exemplifying time-history of the storey drift angle for a given accelerogram.

where  $P_{L,R}$  is the reference probability of exceedance (10%) and  $P_L$  is the probability of exceedance of 2%.

## 7.2. Response parameters

Several response parameters are analysed in order to select a proper value of the behaviour factor. The seismic performance on the occurrence of seismic events with 10% and 2% probabilities of exceedance in 50 years is evaluated at each storey in terms of the brace ductility demand, strength demand of non-dissipative members (beams and columns of the braced frame and gravity columns) and residual drift. EC8 does not stipulate any requirement on residual drift. However, this response parameter is also investigated in this paper because some researchers [29,48] argue that the low post-yield stiffness of BRBs may make frames with BRBs vulnerable to large permanent drifts.

For each nonlinear dynamic analysis, the (maximum) required ductility demand of the braces  $\mu_{Req}$  is determined as the ratio of the maximum axial elongation/shortening to the axial elongation at yielding. The required ductility demand is compared to a reference level of ductility demand  $\mu_{Ref}$ . For seismic events with a probability of exceedance of 2% in 50 years, this reference level is set equal to the ductility capacity  $\mu_{max}$  (achievement of Near Collapse limit state), which has been defined in design as a function of the storey drift angle  $\Delta^d$ . For seismic events with a probability of exceedance of 10% in 50 years, the reference level is set equal to  $3/4 \mu_{max}$  (Significant Damage limit state), similarly to what is stipulated in EC8 – Part 3 [37] for the plastic rotation capacity of members in flexure. Values of the normalised ductility demands  $\bar{\mu} = \mu_{Req}/\mu_{Ref}$  greater than 1 indicate that the brace ductility demand is greater than the reference value.

According to capacity design principles, beams and columns of braced frames and gravity columns should remain elastic during earthquakes and, therefore, their internal forces should not cause instability or yielding. At each instant  $t$  of the time-history response, the members above are subjected to combined axial force  $N(t)$  and bending moment  $M(t)$ . The bending moment acts about one of the principal axes of the cross-section because the model is plane. For bending about the strong axis (y-axis according to EC3 [41]), a stability index (IS) and resistance index (IR) are calculated as

$$IS = \max \left\{ \frac{N(t)}{N_{b,Rd,y}} + k_{yy} \frac{M(t)}{M_{Rd,y}}, \frac{N(t)}{N_{b,Rd,z}} \right\} \quad (27)$$

$$IR = \begin{cases} \frac{M(t)}{M_{Rd,y}} & : \text{ if } \frac{N(t)}{N_{Rd}} \leq 0.5a \\ \frac{N(t)}{N_{Rd}} + (1 - 0.5a) \frac{M(t)}{M_{Rd,y}} & : \text{ if } \frac{N(t)}{N_{Rd}} > 0.5a \end{cases} \quad (28)$$

Instead, for bending about the weak axis (z-axis)

$$IS = \frac{N(t)}{N_{b,Rd,z}} + k_{zz} \frac{M(t)}{M_{Rd,z}} \quad (29)$$

$$IR = \begin{cases} \frac{M(t)}{M_{Rd,z}} & : \text{ if } \frac{N(t)}{N_{Rd}} \leq a \\ \left( \frac{N(t)/N_{Rd} - a}{1 - a} \right)^2 + \frac{M(t)}{M_{Rd,z}} & : \text{ if } \frac{N(t)}{N_{Rd}} > a \end{cases} \quad (30)$$

In the equations above, which are derived from the design rules stipulated in EC3,  $N_{b,Rd,y}$ ,  $N_{b,Rd,z}$ ,  $M_{Rd,y}$  and  $M_{Rd,z}$  are the buckling and plastic moment resistances about the strong and weak axes,  $k_{yy}$  and  $k_{zz}$  are the interaction factors considered in the Method 2 in Annex B of EC3 [41],  $N_{Rd}$  is the plastic resistance to normal forces and  $a$  is the ratio of web area to gross area of the cross-section. All the resistances are calculated according to the design provisions of EC3 assuming that the partial safety factors  $\gamma_{M0}$  and  $\gamma_{M1}$  are equal to unity. Beams and columns do not exceed the limit states of Significant Damage and Near Collapse if both the stability and resistance indexes are lower than unity during seismic events with a probability of exceedance of 10% and 2% in 50 years.

The residual drift angles  $\Delta^{Res}$ , i.e. the ratio of the residual drift to the interstorey height, are also calculated as response parameters. To this

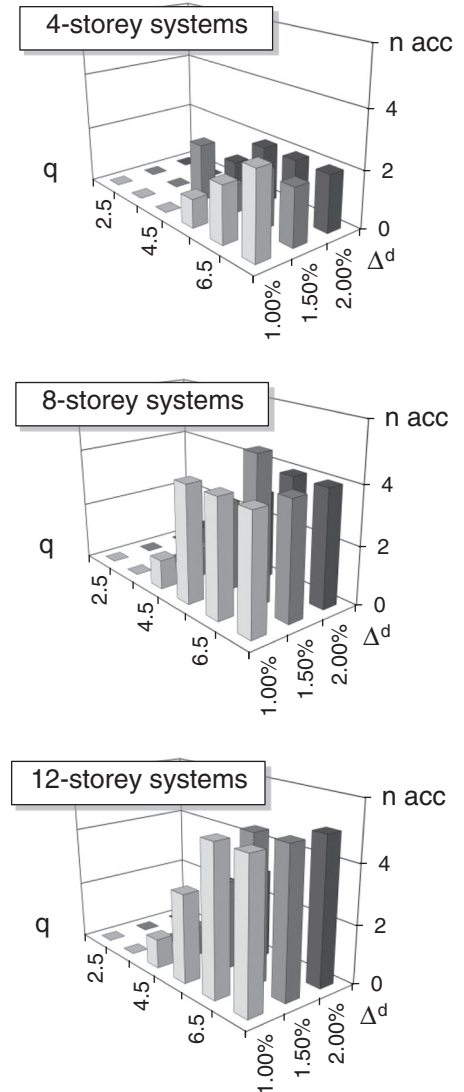


Fig. 7. Number of accelerograms for which numerical instability occurs (systems with non-continuous column; seismic events with probability of exceedance of 2% in 50 years).

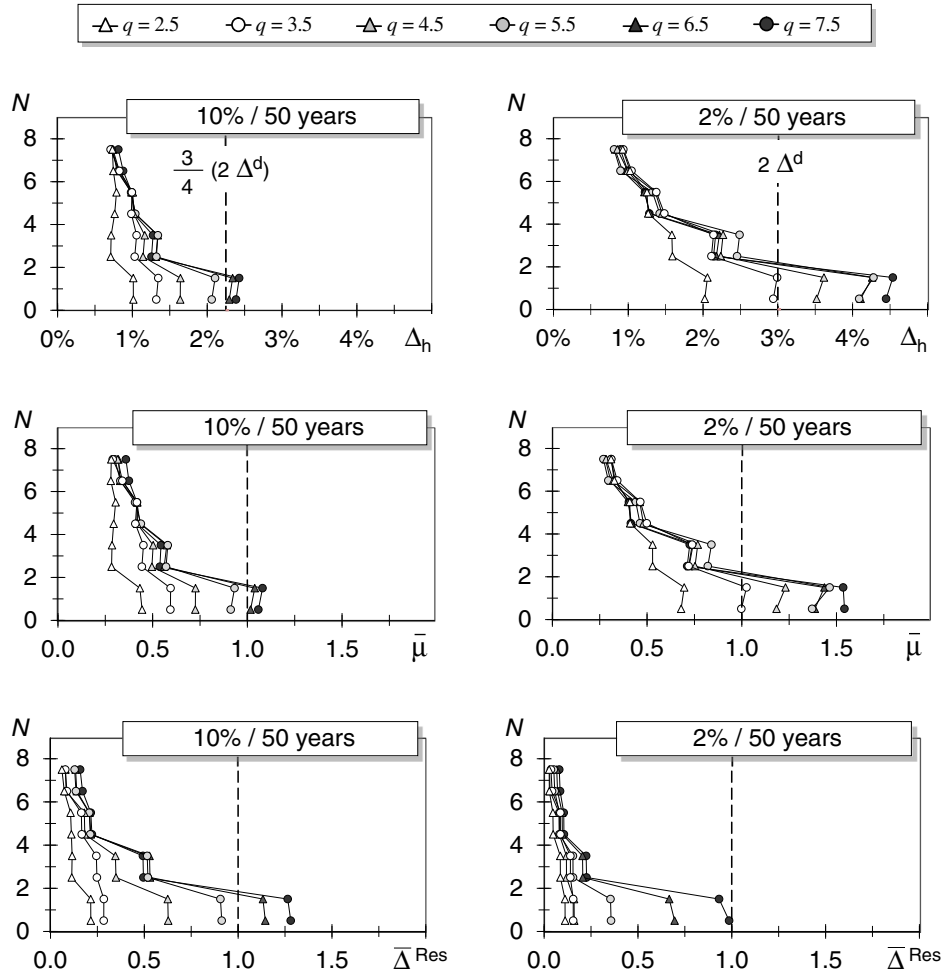


Fig. 8. Heightwise distribution of drift angle, ductility demand in braces and residual drift angle (8-storey systems with non-continuous column,  $\Delta^d = 1.5\%$ ).

end, some zero acceleration points have been added at the end of each accelerogram for an additional duration  $\Delta t_a = 5 T_1$ , where  $T_1$  is the fundamental period of vibration of the analysed system. Then, the residual drift angles are calculated as the mean of the storey drift angle  $\Delta(t)$  in a space of time  $t_f$  equal to  $2 T_1$  from the end of the accelerogram. Fig. 6 illustrates the calculation of the residual drift angle for a given accelerogram. No limit values are provided in EC8 for the residual drift angles. For this reason, the values suggested in the FEMA 356 document [49] for steel braced frames are considered in this paper. According to this code, the Life Safety and Collapse Prevention performance levels are fulfilled if the residual drift angle is lower than 0.5% and 2.0%, respectively. These values are considered here for the limit states of Significant Damage and Near Collapse. The residual drift angles  $\Delta^{\text{Res}}$  obtained for seismic events with a probability of exceedance of 10% and 2% in 50 years are normalised to 0.5% and 2.0%, respectively. Values of the normalised residual drift angles  $\bar{\Delta}_{\text{max}}^{\text{Res}}$  larger than 1 correspond to systems that exceed the relevant limit state.

## 8. Seismic response of the buildings

In this section, the seismic the performance of each building is represented by the median response obtained from the twenty ground motions. For the systems endowed with non-continuous columns and subjected to earthquakes with probability of exceedance of 2% in 50 years, numerical instability occurred in some cases (the number in shown in Fig. 7) and the analysis terminated before the end of the

accelerogram. The structural response to these accelerograms has not been considered for the calculation of the median response.

As an example of the results of all the numerical analyses, Fig. 8 reports the maximum drift angles  $\Delta_h$ , the normalised brace ductility demands and the normalised residual drift angles of some 8-storey systems with non-continuous columns. The hidden lines superimposed to the maximum drift angles, which correspond to drift angles equal to  $3/4 (2 \Delta^d)$  and  $2 \Delta^d$ , represent approximately the attainment of the Significant Damage and Collapse Prevention limit states. The systems are designed with different values of the behaviour factor and a storey drift angle  $\Delta^d$  equal to 1.5%. The numerical analyses show that, if seismic events with probability of exceedance of 10% in 50 years are considered, the normalised ductility demand is greater than 1.0 at the lower storeys of the systems designed by behaviour factors equal to 6.5 and 7.5. So, these systems do not fulfil the Significant Damage limit state requirements. The same conclusion holds if the seismic response is investigated in terms of the normalised residual drift angle. Instead, if seismic events with probability of exceedance of 2% in 50 years are considered, the maximum normalised ductility demand is close to 1.0 in systems designed by behaviour factor equal to 3.5. The normalised residual drifts resulting from these ground motions are always lower than 1.0. It is notable that the analysis of the maximum drift angles leads to the same conclusions obtained from the analysis of normalised ductility demand.

Still referring to the 8-storey systems above, but in the case of continuous columns, Fig. 9 reports the stability index and resistance index of the columns of the braced frame. These indexes are sometimes slightly larger than 1.0 if seismic events with probability of exceedance of 2%

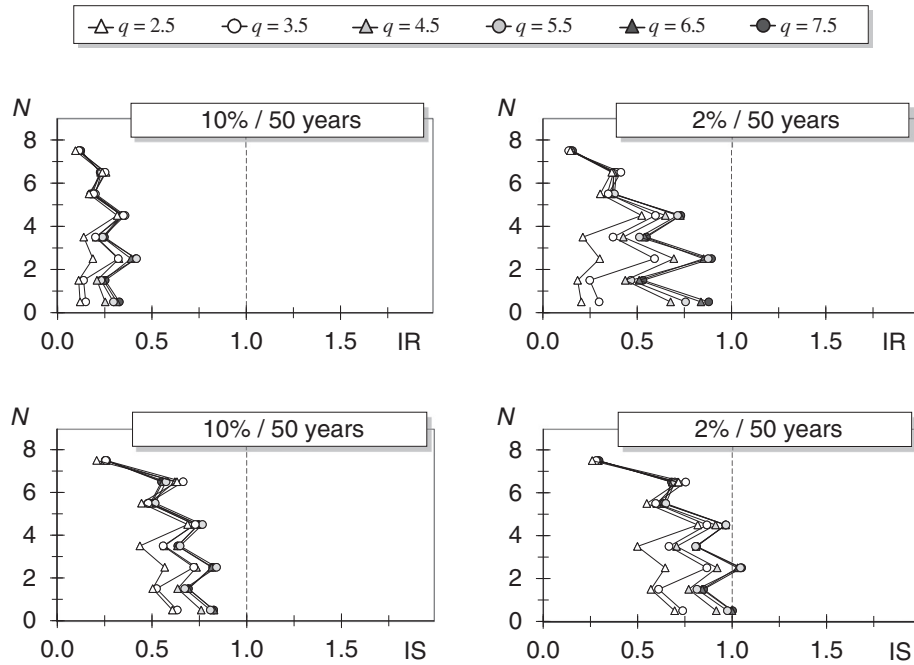


Fig. 9. Heightwise distribution of resistance and stability indexes (8-storey systems with continuous column,  $\Delta^d = 1.5\%$ ).

in 50 years are considered. In these systems, and generally in high-rise systems, the normalised ductility demands of braces are not uniform in elevation and the axial forces transmitted by braces to columns are high at a few storeys only. As a consequence, in these systems the design axial forces are conservatively estimated for columns and significant bending moments are sustained without member instability being triggered. On the contrary, not shown in any figure, the stability index is often larger than 1.0 in the 4-storey systems. In these cases, in fact, the maximum normalised ductility demands of the BRBs are experienced at virtually the same time because the response of these systems is mainly governed by the first mode of vibration. Hence, during the ground motion, columns experience a maximum axial force close to the design value and exceed the target limit state, even in the presence of a moderate bending moment. The same indexes are always lower than 1.0 in the buildings with non-continuous columns.

The maximum values of  $\bar{\mu}$ ,  $\bar{\Delta}^{\text{Res}}$ , IS and IR along the height of the structure are calculated for each case and plotted as a function of the corresponding value of  $q$ . As an example, Fig. 10 reports the results obtained for the 8-storey systems designed for a storey drift angle  $\Delta^d$  equal to 1.5%. When the results are expressed in terms of the stability and resistance indexes of the non-dissipative members, five curves are reported. These curves refer to beams, columns of the braced frame, gravity columns type CC, CL and columns type CB. Each group of these non-

dissipative members is identified by a different symbol. Except for a few cases, the response parameters increase with the behaviour factor. Hence, the behaviour factors  $q$  corresponding to a unit value of the abovementioned response parameters have been calculated for each system by linear interpolation and reported in Tables 7 and 8 with regard to seismic events with probability of exceedance of 10% and 2% in 50 years, respectively. In these tables, the minimum value of the behaviour factors deemed to be acceptable for each system is reported in bold type so as to highlight the response parameter that mainly governs the seismic performance of the system. Some of the systems are characterised by normalised values of the response parameter lower than 1 for all the considered behaviour factors. In these cases, no value of the behaviour factor is reported. In the same tables, the value of  $q^{\text{up}}$  defined in Section 4 is also reported.

If the Significant Damage limit state requirements are considered (see Table 7), the minimum behaviour factors of buildings with continuous columns always correspond to the achievement of the reference brace ductility demand if a design storey drift angle equal to 1% or 1.5% is considered in design. If a storey drift angle equal to 2% is considered, all the examined behaviour factors lead to the fulfilment of the requirements of EC8. In these latter cases, however, the adoption of behaviour factors greater than  $q^{\text{up}}$  are not useful to reduce the size of the member cross-sections significantly. The minimum behaviour

Table 7

Behaviour factor: Significant Damage limit state for probability of exceedance of 10% in 50 years.

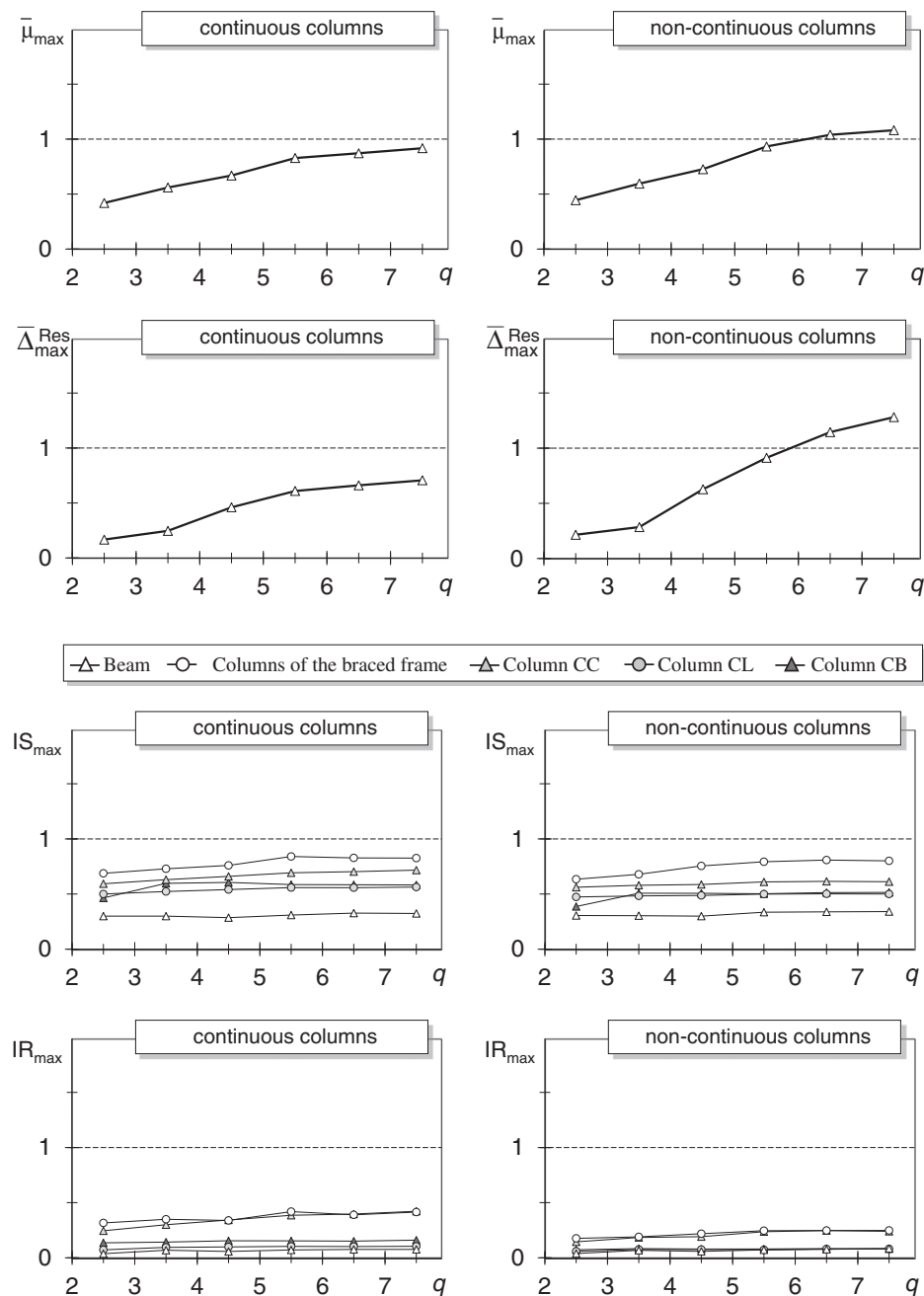
|                |                             | $\Delta^d = 1.0\%$ |             |             | $\Delta^d = 1.5\%$ |             |             | $\Delta^d = 2.0\%$ |             |             |
|----------------|-----------------------------|--------------------|-------------|-------------|--------------------|-------------|-------------|--------------------|-------------|-------------|
|                |                             | $N = 4$            | $N = 8$     | $N = 12$    | $N = 4$            | $N = 8$     | $N = 12$    | $N = 4$            | $N = 8$     | $N = 12$    |
| Non-continuous | $q^{\text{up}}$             | 6.39               | 5.90        | 4.85        | 6.36               | 5.93        | 4.88        | 6.36               | 5.97        | 4.93        |
|                | $\bar{\mu}$                 | <b>4.61</b>        | <b>3.86</b> | <b>3.76</b> | <b>6.73</b>        | 6.13        | (*)         | (*)                | (*)         | (*)         |
|                | $\bar{\Delta}^{\text{Res}}$ | (*)                | 5.85        | 4.24        | (*)                | <b>5.88</b> | <b>4.32</b> | (*)                | <b>5.98</b> | <b>4.40</b> |
|                | IR                          | (*)                | (*)         | (*)         | (*)                | (*)         | (*)         | (*)                | (*)         | (*)         |
|                | IS                          | (*)                | (*)         | (*)         | (*)                | (*)         | (*)         | (*)                | (*)         | (*)         |
| Continuous     | $\bar{\mu}$                 | <b>4.63</b>        | <b>4.37</b> | <b>4.20</b> | <b>7.28</b>        | (*)         | (*)         | (*)                | (*)         | (*)         |
|                | $\bar{\Delta}^{\text{Res}}$ | (*)                | (*)         | (*)         | (*)                | (*)         | (*)         | (*)                | (*)         | (*)         |
|                | IR                          | (*)                | (*)         | (*)         | (*)                | (*)         | (*)         | (*)                | (*)         | (*)         |
|                | IS                          | (*)                | (*)         | (*)         | (*)                | (*)         | (*)         | (*)                | (*)         | (*)         |

(\*) All the considered values of  $q$  lead to a seismic demand lower than the corresponding capacity.

**Table 8**

Behaviour factor: Near Collapse limit state for probability of exceedance of 2% in 50 years.

|                |                      | $\Delta^d = 1.0\%$ |             |             | $\Delta^d = 1.5\%$ |             |             | $\Delta^d = 2.0\%$ |             |             |
|----------------|----------------------|--------------------|-------------|-------------|--------------------|-------------|-------------|--------------------|-------------|-------------|
|                |                      | $N = 4$            | $N = 8$     | $N = 12$    | $N = 4$            | $N = 8$     | $N = 12$    | $N = 4$            | $N = 8$     | $N = 12$    |
| Non-continuous | $q^{up}$             | 6.39               | 5.90        | 4.85        | 6.36               | 5.93        | 4.88        | 6.36               | 5.97        | 4.93        |
|                | $\bar{\mu}$          | <b>2.88</b>        | <b>2.50</b> | <b>2.50</b> | <b>4.60</b>        | <b>3.42</b> | <b>3.56</b> | <b>5.68</b>        | <b>5.08</b> | (*)         |
|                | $\bar{\Delta}_{Res}$ | (*)                | (*)         | (*)         | (*)                | (*)         | (*)         | (*)                | (*)         | (*)         |
|                | IR                   | (*)                | (*)         | (*)         | (*)                | (*)         | (*)         | (*)                | (*)         | (*)         |
| Continuous     | IS                   | 6.63               | (*)         | (*)         | (*)                | (*)         | (*)         | (*)                | (*)         | (*)         |
|                | $\bar{\mu}$          | <b>2.87</b>        | <b>2.55</b> | <b>2.50</b> | 4.43               | <b>3.89</b> | <b>4.22</b> | 6.38               | 6.64        | (*)         |
|                | $\bar{\Delta}_{Res}$ | (*)                | (*)         | (*)         | (*)                | (*)         | (*)         | (*)                | (*)         | (*)         |
|                | IR                   | 5.73               | (*)         | (*)         | 5.81               | (*)         | (*)         | 5.77               | (*)         | (*)         |
|                |                      | IS                 | 3.37        | 4.25        | 4.40               | <b>3.19</b> | 5.14        | (*)                | <b>3.97</b> | <b>5.90</b> |

(\*) All the considered values of  $q$  lead to a seismic demand lower than the corresponding capacity.**Fig. 10.** Evaluation of the maximum behaviour factor (8-storey systems,  $\Delta^d = 1.5\%$ , seismic events with probability of exceedance of 10% in 50 years).

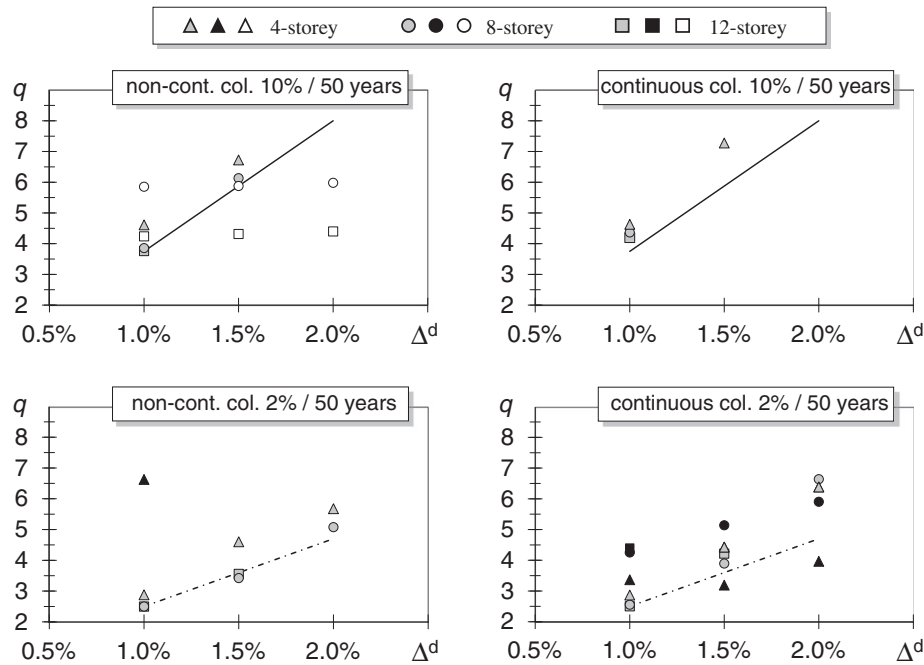


Fig. 11. Proposed behaviour factors.

factors of buildings with non-continuous columns correspond to the achievement of residual drift angles greater than the reference limit if the design storey drift angles are equal to 1.5% or 2.0%. Even if this response parameter is not explicitly checked in EC8, the writers suggest considering this parameter when selecting a proper value of the behaviour factor. The obtained values of the behaviour factor generally decrease with the increase in the height of the building. This finding is consistent with the results of other studies concerning the evaluation of the response modification factor of frames endowed with BRBs [23, 25,24] or other braced frames [45,50–54]. However, the values of  $q$  obtained here are much lower than those reported in [23–25], especially in the 4-storey systems.

If the Near Collapse limit state requirement is considered (see Table 8), the minimum behaviour factors are due to the achievement of the reference brace ductility demand. Specifically, behaviour factors close to 2.5 are obtained for systems designed for  $\Delta^d = 1.0\%$ . The limits on the residual drifts are never restrictive. Only occasionally (low-storey systems designed for  $\Delta^d = 1.5\%$  or  $\Delta^d = 2.0\%$ ) the value of the behaviour factor is limited because of the stability index of the columns of the braced frames. Based on these results, if the Near Collapse requirement has to be fulfilled, steel frames with BRBs designed by  $\Delta^d$  not lower than 1.5% should be preferred to avoid the use of low values of the behaviour factor and, therefore, large design seismic forces.

## 9. Proposal of the behaviour factor

To define a relation between the design storey drift angle  $\Delta^d$  and the maximum acceptable behaviour factor  $q_{\max}$ , the values of the behaviour factor previously determined are reported in Fig. 11 as a function of  $\Delta^d$ . A different symbol (triangle, circle or square) is used to pinpoint systems characterised by a different number of storeys (4, 8 or 12). A different colour is adopted to highlight the response parameter that leads to the selected value of  $q_{\max}$ . Specifically, a grey symbol is used for the normalised ductility demand, a black symbol for the stability index of all the non-dissipative members and a white symbol for the normalised residual drift angle.

For each of the two considered target performance levels, an analytical equation is proposed to determine a proper value of the behaviour factor  $q_{\max}$  as a function of the design storey drift angle  $\Delta^d$ . These

equations are reported in Table 9 and are determined ignoring the requirements on the residual drift. The values  $q_{\max}$  obtained from these relations are represented in Fig. 11 along with those evaluated by numerical analysis. The equation of the behaviour factor which has been determined from the fulfilment of the Near Collapse requirement ( $q_{\max}^{(2\%)}$ , dot-dashed line) provides values that increase with  $\Delta^d$  and range from 2.5 to 4.7. These values of  $q_{\max}$  are always lower than those obtained from the equation referring to the Significant Damage requirement ( $q_{\max}^{(10\%)}$ , continuous line), which range from 3.75 to 8.0. Therefore,  $q_{\max}^{(2\%)}$  is suggested for the evaluation of the behaviour factor to be used for design of steel frames with BRBs to fulfil both the Significant Damage and the Collapse Prevention limit state in the occurrence of the relevant ground motions.

The values of  $q_{\max}$  obtained by the proposed equation are rather small if the assumed value of  $\Delta^d$  is lower than 1.5%. For instance,  $q_{\max}$  is equal to 2.5 for  $\Delta^d = 1.0\%$ . This value is the same adopted in EC8 for high ductility chevron bracings, which is among of the lowest values of  $q$  suggested in EC8 for steel building structures. Based on this consideration, a minimum value of 1.5% is suggested for  $\Delta^d$ . Furthermore, it is notable that even if very ductile BRBs are used (i.e.,  $\Delta^d = 2.0\%$  is adopted), the proposed equation provides a behaviour factor equal to 4.7. This value is large, but it is still well below that stipulated in EC8 for high ductility moment resisting frames, which can attain the value of 6.5.

Finally, an upper limit of  $q_{\max}$  should be considered for the 12-storey systems if the fulfilment of the Significant Damage is required also in terms of the residual storey drift. In particular, a behaviour factor not larger than 4 has to be adopted to avoid that 12-storey systems with non-continuous columns exceed the Significant Damage limit state for ground motions with 10% probability of exceedance in 50 years (white squares in Fig. 11).

**Table 9**  
Proposed behaviour factors for  $\Delta^d \leq 2.0\%$ .

| Significant Damage<br>(10% in 50 years)          | Near Collapse<br>(2% in 50 years)             |
|--|---|
| $q_{\max}^{(10\%)} = 425 \Delta^d (\%) - 0.50^a$ | $q_{\max}^{(10\%)} = 220 \Delta^d (\%) + 0.3$ |

<sup>a</sup> A maximum value of  $q_{\max}^{(10\%)}$  equal to 4 is suggested to limit the residual drift angle.

## 10. Considerations on the limit state of damage limitation

According to EC8, the damage produced by the seismic action associated with the Damage Limitation requirement is acceptable if the maximum storey drift is lower than an assigned limit value. This limit is fixed depending on the type of connection between structural and non-structural elements and ranges from 0.005 to 0.010 times the interstorey height. The fulfilment of the Damage Limitation requirement was not checked in design. For this reason, the maximum storey drift required by a set of accelerograms corresponding to a probability of exceedance of 50% in 50 years is calculated. This set of accelerograms is obtained by scaling of the accelerograms with 10% probability of exceedance in 50 years. The scale factor  $SF$ , equal to 0.58, is calculated by means of Eq. (26). The maximum demand of storey drift angle ( $\Delta_{\max}$ ) of the buildings is plotted as a function of the behaviour factor adopted in design and is shown in Fig. 12 with regard to the examined 4- and 12-storey systems with non-continuous columns. In the same figure, the values of the storey drift angle  $\Delta_{\max}$  corresponding to the use of the proposed behaviour factors (those provided by the equation corresponding to the fulfilment of the Near Collapse requirement) are also highlighted. The figure shows that the proposed values of the behaviour factor lead to systems characterised by maximum storey drift angles  $\Delta_{\max}$  from 0.5% to 1.0%. These considerations also apply to systems with continuous columns, even if in these cases the values of  $\Delta_{\max}$  are slightly lower than those of systems with non-continuous columns. These results further demonstrate that the adoption of the proposed values of the behaviour factor is appropriate, because it leads to systems that

also fulfil the Damage Limitation requirement. Further, the adoption of larger values of  $q$  would lead to very flexible systems that could fail the Damage Limitation requirement. In this case, the frame needs to be stiffened and the suggested behaviour factor may be illusory.

## 11. Conclusions

The paper describes a procedure for the seismic design of steel frames equipped with BRBs. The procedure is consistent with the framework of EC8 because it is chiefly derived from that reported in this code for steel chevron braced frames. Braces are designed for resistance and ductility to dissipate the input seismic energy while beams and columns are designed to remain elastic by means of rules for the application of the capacity design principles. The application of the capacity design principles requires the evaluation of the tension and compression strength adjustment factors  $\omega$  and  $\beta$ . Based on the results of a wide set of experimental test results, an analytical relation of the parameter  $\omega$  is determined as a linear function of the expected maximum ductility demand of BRBs. The analysis of the same test results also shows that  $\beta$  may be given a single value equal to 1.1. It is notable that the obtained values of  $\omega$  and  $\beta$  may be helpful for any design or assessment procedure that requires the evaluation of the maximum axial force transmitted by BRBs to the backup frame.

The design procedure is applied to a large set of buildings that are subjected to seismic ground motions with 2%, 10% and 50% probabilities of exceedance in 50 years. The results of the numerical investigation, which refer to design storey drift angles not larger than 2%, are used

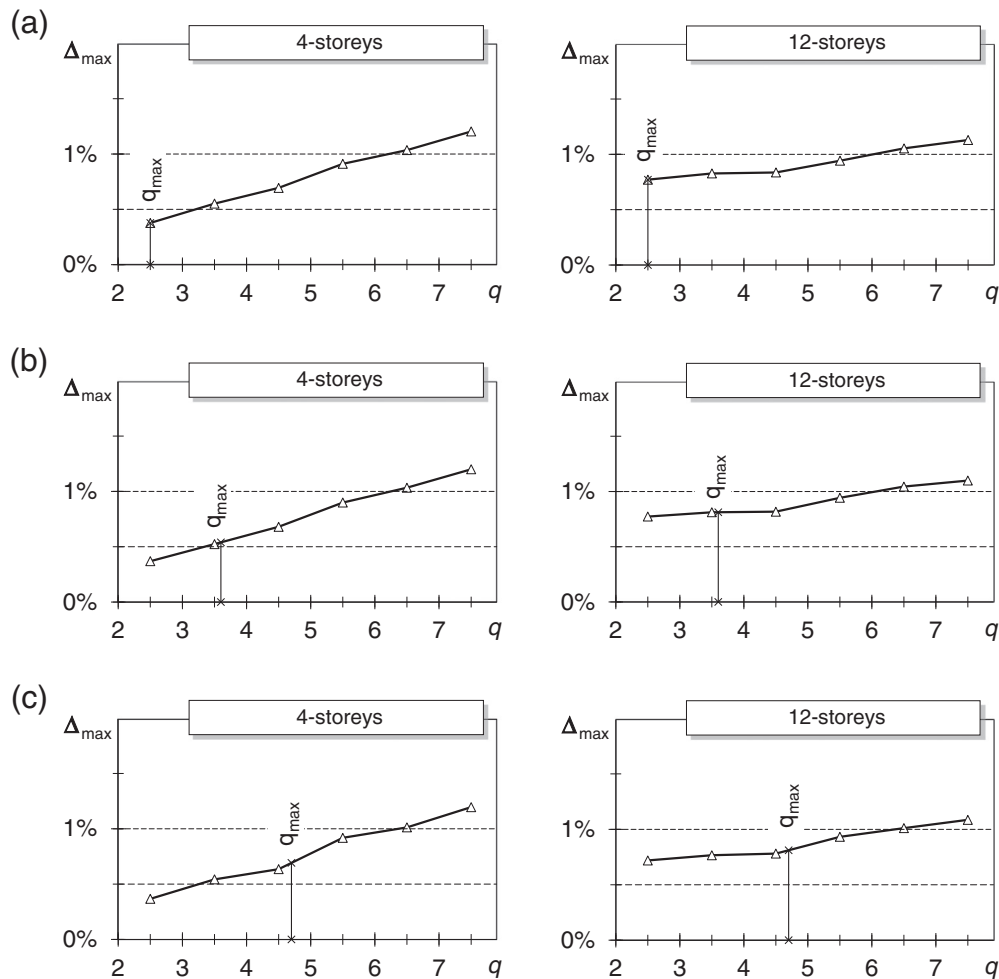


Fig. 12. Maximum storey drift angle for seismic events with probability of exceedance of 50% in 50 years: systems with non-continuous columns designed by  $\Delta^d$  equal to (a) 1.0%, (b) 1.5% and (c) 2.0%.

to define the behaviour factor  $q$  as a function of the design storey drift angle  $\Delta^d$ . The main conclusions on the behaviour factor to be adopted are resumed in the following.

- The maximum acceptable behaviour factor increases with the design storey drift angle and is slightly beneficially affected by the presence of continuous columns.
- The fulfilment of the Near Collapse requirement is generally responsible for the value of the proposed behaviour factor. The proposed behaviour factor linearly varies with the design storey drift angle and ranges from 2.5 (for  $\Delta^d = 1.0\%$ ) to 4.7 (for  $\Delta^d = 2.0\%$ ). If non-continuous columns are considered, an upper value equal to 4 is suggested to limit the residual storey drifts.
- A minimum design storey drift angle equal to 1.5% is suggested to avoid the use of a rather low value of the behaviour factor (2.5). If non-continuous columns are considered, a design storey drift angle higher than 1.5% is not helpful because of the upper limit of the behaviour factor ( $q = 4$ ).
- The adoption of the proposed values of the behaviour factor leads to systems that satisfy also the Damage Limitation requirement. Therefore, the proposed behaviour factors represent an optimal solution for the design of steel frames with BRBs, because they allow the fulfilment of all the performance requirements stipulated in EC8.

## References

- [1] G. Della Corte, M. D'Aniello, R. Landolfo, F.M. Mazzolani, Review of steel buckling-restrained braces, *Steel Constr* 4 (2) (2011) 85–93.
- [2] Q. Xie, State of the art of buckling-restrained braces in Asia, *J Constr Steel Res* 61 (2005) 727–748.
- [3] C.M. Uang, M. Nakashima, *Earthquake Engineering: From Engineering Seismology to Performance Based Engineering*, CRC Press LLC, 2004.
- [4] C.J. Black, N. Makris, I.D. Aiken, Component testing, stability analysis and characterization of buckling restrained 'unbonded' braces, Technical Report PEER 2002/08, Pacific Earthquake Engineering Research Center, University of California, Berkeley, 2002.
- [5] G. Della Corte, M. D'Aniello, R. Landolfo, Field testing of all-steel buckling-restrained braces applied to a damaged reinforced concrete building, *J Struct Eng ASCE* 141 (1) (2015) (paper D4014004).
- [6] L.A. Fahnestock, R. Sauce, J.M. Ricles, L.W. Lu, Ductility demands on buckling-restrained braced frames under earthquake loading, *Earthq Eng Eng Vib* 2 (2) (2003) 255–268.
- [7] M. Iwata, T. Kato, A. Wada, Performance evaluation of buckling restrained braces in damage-controlled structures, in: F.M. Mazzolani (Ed.), *Behavior of Steel Structures in Seismic Areas*, Proceedings of the 4th International Conference STESSA 2003 2003, pp. 37–43 (Naples, Italy).
- [8] M. Iwata, T. Kato, A. Wada, Buckling restrained braces as hysteretic dampers, in: F.M. Mazzolani, R. Tremblay (Eds.), *Behavior of Steel Structures in Seismic Areas*, Proceedings of the 3rd International Conference STESSA 2000 2000, pp. 33–38 (Montreal, Canada).
- [9] M. Iwata, M. Murai, Buckling-restrained brace using steel mortar planks; performance evaluation as a hysteretic damper, *Earthq Eng Struct Dyn* 35 (2006) 1807–1826.
- [10] S. Merritt, C.M. Uang, G. Benzoni, Subassemblage testing of core brace buckling restrained braces, Structural Systems Research Project, Report No. TR-2003/01, University of California, San Diego, 2003.
- [11] S. Merritt, C.M. Uang, G. Benzoni, Subassemblage testing of star seismic buckling restrained braces, Structural Systems Research Project, Report No. TR-2003/04, University of California, San Diego, 2003.
- [12] J. Newell, C.M. Uang, G. Benzoni, Subassemblage testing of corebrace buckling restrained braces (G series), Structural Systems Research Project, Report No. TR-2006/01, University of California, San Diego, 2006.
- [13] T. Usami, A. Kasai, M. Kato, Behavior of buckling-restrained brace members, in: F. Mazzolani (Ed.), *Behavior of Steel Structures in Seismic Areas*, Proceedings of the 4th International Conference STESSA 2003 2003, pp. 211–216 (Naples, Italy).
- [14] J. Zhao, B. Wu, J. Ou, A novel type of angle steel buckling-restrained brace: cyclic behavior and failure mechanism, *Earthq Eng Struct Dyn* 40 (2011) 1083–1102.
- [15] G. Brando, G. De Matteis, Design of low strength-high hardening metal multi-stiffened shear plates, *Eng Struct* 60 (2014) 2–10.
- [16] A. Formisano, G. De Matteis, F.M. Mazzolani, Numerical and experimental behaviour of a full-scale RC structure upgraded with steel and aluminium shear panels, *Comput Struct* 88 (2010) 1348–1360.
- [17] T. Okazaki, M.D. Engelhardt, Cyclic loading behavior of EBF links constructed of ASTM A992 steel, *J Construct Steel Res* 63 (2007) 751–765.
- [18] CEN, EuroCode 8: Design of Structures for Earthquake Resistance — Part 1: General Rules, Seismic Actions and Rules for Buildings, European Committee for Standardization, Bruxelles, 2005.
- [19] Federal Emergency Management Agency, FEMA 450, NEHRP Recommended Provisions for Seismic Regulations for New Buildings and Other Structures, Washington, D.C., USA2004.
- [20] AISC 2005, Seismic Provision for Structural Steel Buildings, American Institute of Steel Construction, Chicago, 2005.
- [21] R. Sabelli, S.A. Mahin, C. Chang, Seismic demands on steel braced frame buildings with buckling-restrained braces, *Eng Struct* 25 (2003) 655–666.
- [22] L.A. Fahnestock, R. Sauce, J.M. Ricles, Seismic response and performance of buckling restrained braced frame, *J Struct Eng (ASCE)* 133 (9) (2007) 1195–1204.
- [23] B. Asgarian, H.R. Shokrgozar, BRBF response modification factor, *J Construct Steel Res* 65 (2009) 290–298.
- [24] J. Kim, J. Park, S. Kim, Seismic behavior factors of buckling restrained braced frames, *Struct Eng Mech* 33 (3) (2009) 261–284.
- [25] M. Mahmoudi, M. Zaree, Evaluating response modification factors of concentrically braced steel frames, *J Constr Steel Res* 66 (2010) 1196–1204.
- [26] M. Bosco, A. Ghersi, E.M. Marino, On the evaluation of seismic response of structures by nonlinear static methods, *Earthq Eng Struct Dyn* 38 (2009) 1465–1482.
- [27] A.K. Chopra, R.K. Goel, A modal pushover analysis procedure for estimating seismic demands for buildings, *Earthq Eng Struct Dyn* 31 (2002) 561–582.
- [28] A.M. Mwafy, A.S. Elnashai, Static pushover versus dynamic collapse analysis of RC buildings, *Eng Struct* 23 (2001) 407–424.
- [29] S. Kiggins, C.M. Uang, Reducing residual drift of buckling-restrained braced frames as a dual system, *Eng Struct* 28 (2006) 1525–1532.
- [30] L. Di Sarno, A.S. Elnashai, Bracing systems for seismic retrofitting of steel frames, *J Constr Steel Res* 65 (2009) 452–465.
- [31] K. Deng, P. Pan, A. Lam, Y. Xue, A simplified model for analysis of high-rise buildings equipped with hysteretic damped outriggers, *Struct Des Tall Special Build* 23 (15) (2014) 1158–1170.
- [32] P.P. Rossi, Importance of isotropic hardening in the modeling of buckling restrained braces, *J Struct Eng (ASCE)* 14 (4) (2015) (04014124(1–11)).
- [33] A. Zona, A. Dall'Asta, Elastoplastic model for steel buckling-restrained braces, *J Constr Res* 68 (1) (2012) 118–125.
- [34] S. Mazzoni, F. McKenna, M.H. Scott, G.L. Fenves, et al., *OpenSees Command Language Manual*, 2007.
- [35] G. Brandonisio, M. Toreno, E. Grande, E. Mele, A. De Luca, Seismic design of concentric braced frames, *J Constr Steel Res* 78 (2012) 22–37.
- [36] E.M. Marino, A unified approach for the design of high ductility steel frames with concentric braces in the framework of Eurocode 8, *Earthq Eng Struct Dyn* 43 (2014) 97–118.
- [37] CEN, EuroCode 8: Design of Structures for Earthquake Resistance — Part 3: Assessment and Retrofitting of Buildings, European Committee for Standardization, Bruxelles, 2005.
- [38] M. Bosco, E.M. Marino, Design method and behavior factor for steel frames with buckling restrained braces, *Earthq Eng Struct Dyn* 42 (2013) 1243–1263.
- [39] F. Amara, M. Bosco, E.M. Marino, P.P. Rossi, An accurate strength amplification factor for the design of SDOF Systems with P–Δ Effects, *Earthq Eng Struct Dyn* 43 (2014) 589–611.
- [40] R. Tremblay, L. Poncet, P. Bolduc, R. Neville, R. De Vall, Testing and design of buckling restrained braces for Canadian application, Proceedings of the World Conf. on Earthquake Engineering, Int. Association for Earthquake Engineering, Tokyo, Japan 2004, pp. 1–15.
- [41] CEN, EuroCode 3: Design of Steel Structures — Part 1-1: General Rules and Rules for Buildings, ENV 1993-1-1, European Committee for Standardization, Bruxelles, 2005.
- [42] C. Ariyaratana, L.A. Fahnestock, Evaluation of buckling-restrained braced frames seismic performance considering reserve strength, *Eng Struct* 33 (2011) 77–89.
- [43] X. Ji, M. Kato, T. Wang, T. Hitaka, M. Nakashima, Effect of gravity columns on mitigation of drift concentration for braced frames, *J Constr Steel Res* 65 (2009) 2148–2156.
- [44] G.A. MacRae, Y. Kimura, C. Roeder, Effect of column stiffness on braced frame seismic behaviour, *J Struct Eng ASCE* 130 (3) (2004) 381–391.
- [45] R. Tremblay, Achieving a stable inelastic seismic response for multi-story concentrically braced steel frames, *Eng J (AISC)* 40 (2003) 111–129.
- [46] J.M. Ricles, E.P. Popov, Dynamic analysis of seismically resistant eccentrically braced frames, Earthquake Engineering Research Center, Report No. UCB/EERC-87/07, University of California, Berkeley, 1987.
- [47] P.G. Somerville, N.F. Smith, S. Punyamurthula, J.I. Sun, Development of ground motion time histories for phase 2 of the FEMA/Sac steel project, SAC Background Document. Report No. SAC/BD-99-03, SAC Joint Venture, 555 University Ave., Sacramento, 1997.
- [48] J. Erochko, C. Christopoulos, R. Tremblay, H. Choi, Residual drift response of SMRFs and BRB frames in steel buildings designed according to ASCE 7-05, *J Struct Eng (ASCE)* 137 (2011) 589–599.
- [49] FEMA 356, *Prestandard and Commentary for the Seismic Rehabilitation of Buildings*, Federal Emergency Management Agency, Washington, DC, U.S.A., 2000.
- [50] E.M. Marino, M. Nakashima, Seismic performance and new design procedure for chevron-braced frames, *Earthq Eng Struct Dyn* 35 (2006) 433–452.
- [51] M. Bosco, P.P. Rossi, A design procedure for dual eccentrically braced systems: numerical investigation, *J Constr Steel Res* 80 (2013) 453–464.
- [52] M. Bosco, E.M. Marino, P.P. Rossi, Proposal of modifications to the design provisions of Eurocode 8 for buildings with split k eccentric braces, *Eng Struct* 61 (2014) 209–223.
- [53] M. Bosco, P.P. Rossi, Seismic behaviour of eccentrically braced frames, *Eng Struct* 31 (2009) 664–674.
- [54] P.P. Rossi, A. Lombardo, Influence of the link overstrength factor on the seismic behaviour of eccentrically braced frames, *J Constr Steel Res* 63 (11) (2007) 1529–1545.